

International Conference on Space Optics—ICSO 2022

Dubrovnik, Croatia

3–7 October 2022

Edited by Kyriaki Minoglou, Nikos Karafolas, and Bruno Cugny,



Optical Ranging and Time Transfer Calibration on the CubeSat Laser Infrared Crosslink Mission



Optical Ranging and Time Transfer Calibration on the CubeSat Laser Infrared CrosslinK Mission

Paul Serra^a, Hannah Tomio^a, Nicholas Belsten^a, William Kammerer^a, Peter Grenfell^a, Myles Clark^b, Danielle Coogan^b, Joseph Conroy^b, David Mayer^c, Jan Stupl^c, John Hanson^c, Laura Hyst^d, John Conklin^b, and Kerri Cahoy^a

^aDepartment of Aeronautics and Astronautics, MIT, Cambridge, MA, USA

^bDepartment of Mechanical and Aerospace Engineering, University of Florida, Gainesville, FL, USA

^cNASA Ames Research Center, Moffett Field, CA, USA

^dInstitut Supérieur de l'Aéronautique et de l'Espace – SUPAERO, Toulouse, France

ABSTRACT

This work presents a novel calibration method for time transfer and ranging systems. The CLICK-B/C design uses a shared aperture for transmit and receive, and optical isolation is achieved using free-space dichroics and band-pass filters. During calibration, the transmitter is tuned close to the receiver assigned wavelength, bypassing filtering during calibration. The receiver is able to measure the outgoing signal due to internal reflections on the telescope lenses. The transmitter and receiver delays can then be subtracted from time of flight, eliminating delay uncertainties arising from all components of the transmitter and receiver, with minimal change in their operating conditions. Thanks to the high repetition rates of communication links, more than 10 MHz, this method could lead to millimeter-level absolute ranging, as well as time transfer accuracy in the low picoseconds, enabling new applications and advances in space radio interferometry, GPS-denied navigation, and time synchronization for synthetic aperture telescopes.

Keywords: CubeSat, Time transfer, Ranging, Optical communication, Metrology

1. INTRODUCTION

In recent years, constellations or swarms of nanosatellites have emerged as a new mission architecture for a variety of applications, providing global coverage and high revisit rates. High-speed data transfer and precision time transfer, both between the satellites and from space-to-ground, can greatly benefit such missions. Laser communications technologies can enable these capabilities through compact, power-efficient terminals that have lower size, weight, and power (SWaP) than comparable RF systems.^{1,2}

The CubeSat Laser Infrared CrosslinK (CLICK) mission is a joint project with the Massachusetts Institute of Technology (MIT), the University of Florida (UF), and NASA Ames Research Center. Its goal is to demonstrate cost-effective, low size, weight, and power (SWaP) laser communication terminals with the ability to conduct downlinks and crosslinks. The CLICK mission consists of three CubeSats: CLICK-A, CLICK-B, and CLICK-C. CLICK-A launched first, in July 2022, and will serve as a risk-reduction mission that will demonstrate just the space-to-ground downlink capability. CLICK-B and CLICK-C will follow in 2023 and demonstrate the full crosslink and downlink capability. In addition to the communication links, CLICK-B and CLICK-C are also capable of precision ranging and time transfer.

CLICK-B/C will demonstrate crosslinks at ranges between 25 km and 580 km with a data rate of greater than 20 Mbps. Space-to-ground downlinks with data rates of greater than 10 Mbps will also be demonstrated to an

Further author information:
P.S.: E-mail: pserra@mit.edu
H.T.: E-mail: tomio@mit.edu
N.B.: E-mail: nbelsten@mit.edu

optical ground station, the Portable Telescope for LaserCom (PorTeL).³ The CLICK-B/C mission also intends to demonstrate a ranging precision capability of less than 50 cm and a time transfer precision of less than 200 ps single shot. The 1.5U CLICK-B and CLICK-C payloads are identical in design except for transmitting at slightly different wavelengths, 1537 nm and 1563 nm respectively, to facilitate spectral isolation. For the transmitter, they feature a tunable seed laser and a commercial-off-the-shelf (COTS) Erbium-Doped Fiber Amplifier (EDFA). The seed laser is followed by a Semiconductor Optical Amplifier (SOA) acting as a shutter. The SOA modulates the transmitted signal with both data and timing, using Pulse Position Modulation (PPM). The payload receives data and measures time of flight using an Avalanche Photodiode (APD) detector with a 700 MHz bandwidth and programmable gain. CLICK-B/C employs two methods to demodulate the received signal: an Analog-to-Digital Converter (ADC)-based approach with a matched filter and a Time-to-Digital Converter (TDC)-based approach that can be used to recover data and timing simultaneously.

This work assesses the feasibility of a novel calibration method to improve timing and ranging accuracy. It exploits the cross-talk between transmit and received signals on the common parts of the optical path. The level of internal reflections at the receiver's detector can be controlled by adjusting the transmitter wavelength. Optical powers within a range 1×10^{-2} pW to 4 μ W can be achieved, making calibration possible for all the inter-satellite distances, 25 to 580 km, required for the mission.

2. PAYLOAD DESIGN

2.1 Time transfer and ranging operations

Ranging and timing operations on the CLICK-BC payload are based on timestamps. Timestamps are collected both at emission and receptions on each spacecraft, yielding four timestamp for each transfers: t_{TX}^B and t_{RX}^B for transmit and receive on payload B, and, similarly, t_{TX}^C and t_{RX}^C for payload C. Each spacecraft use its own internal clock to measure the timestamps. The clock discrepancy between B and C, noted χ , can then be found with the following equation:

$$\chi = \frac{t_{TX}^C + t_{RX}^C}{2} - \frac{t_{TX}^B + t_{RX}^B}{2} \quad (1)$$

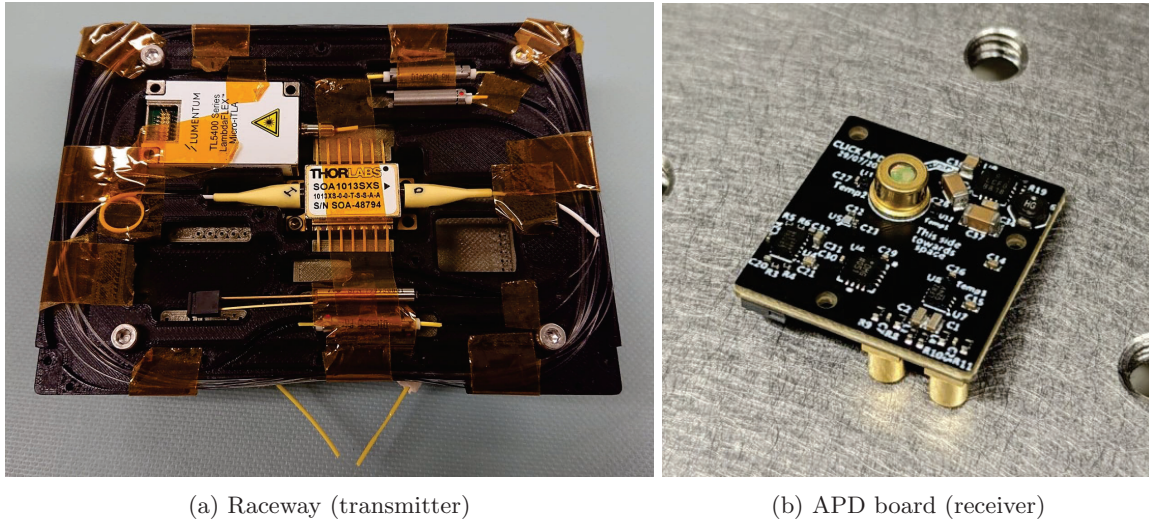
The range between the spacecrafts, noted D , is also derived from the same timestamps:

$$D = \frac{c}{2} (t_{RX}^C - t_{TX}^B + t_{RX}^B - t_{TX}^C) \quad (2)$$

2.2 Transmitter

The transmitter is composed of a seed laser, a Semiconductor Optical Amplifier (SOA) used as a modulator, and a Erbium Doped Fiber Amplifier (EDFA). The CLICK-B/C transmitter uses an identical EDFA to CLICK-A, however the modulation method differs.

The seed laser is a Micro-Integrated Tunable Laser Assembly (μ ITLA). This source is capable of tuning its wavelength, covering the entire infrared C-Band, the range of wavelength compatible with EDFAs. This functionality is exploited in order to calibrate timing using the method described in this work. At the output of the micro-ITLA, the light is attenuated by a few fiber bends. This ensures that the optimal seed power for the SOA is within the adjustment range of the μ ITLA. The optimal power is the SOA input power at which the SOA provides the highest extinction ratio when used as a shutter, targeting 0.1 mW. The SOA modulates the transmitted data, with an expected high level of 1 mW and an extinction ratio in excess of 50 dB. This extinction ratio is sufficient to support modulation orders up to PPM128, with 128 time slots for a pulse, encoding 7 bits per symbol. The SOA is controlled by fully turning on and off the current through it. With the SOA providing the on/off switching, the laser oscillation is not affected by our power modulation method. Since the light does only a single round trip in the SOA, cavity dynamics effects are avoided, which can be a problematic when rapidly turning on laser diodes. The SOA output is connected to a tap photo-detector for diagnostic and SOA control optimization. The seed laser and the SOA are pictured in fig. 1a, installed in a test assembly of the payload raceway. The light is then sent to the EDFA, and is amplified to 200 mW average. At higher PPM orders, implementation loss due to the large duty cycle results in drop of the signal optical power, down to 160 mW average in PPM128.



(a) Raceway (transmitter)

(b) APD board (receiver)

Figure 1: (a) Picture of a CLICK-B/C raceway test assembly showing the transmitter fiber components. The μ ITLA module on the top left is the seed laser, data is modulated by the SOA in center, and amplified by the EDFA mounted at the back of the assembly. (b) Picture of the CLICK-BC detector module. The board is 2.5×2.5 cm. The APD itself is inside the can in the middle.

2.3 Detector

The CLICK-BC detector is composed of an Avalanche Photodiode (APD), followed by two different amplification and filtering chains.^{4,5} A picture of the detector board is shown in fig. 1b.

The high-bandwidth signal chain carries data, with a bandwidth of 20 kHz to 700 MHz. It is composed of the APD integrated trans-impedance amplifier (TIA), two differential programmable gain amplifiers (PGAs), and an offset correction circuit. The trans-impedance amplifier outputs a differential signal proportional to the APD optical power, amplified by the two PGAs in order to cover the full dynamic range expected during the CLICK mission. The offset correction circuit shifts the average differential voltage output of the detector in order to correct for duty cycle of pulse-position modulation. As the PPM signal is not balanced, but rather the inverse of the number of pulse slots for a symbol, the offset is introduced as a form of DC-recovery, to increase the useful signal range.

The other signal chain is used to control the gain and perform diagnostic. The signal is much slower, with a bandwidth from DC to 20 KHz. The signal is obtained by measuring the APD current on the high side, at the bias voltage supply. The bias voltage source includes a current mirror, providing a copy of the APD current. This current is measured by a log-trans-impedance amplifier, covering the entire range of expected APD currents, from dark current at low gain, around 1 nA, to beyond the average current absolute maximum value, at 1 mA. Unlike the fast chain dedicated to data, the signal from this slower chain is sampled in the detector itself with a 12 bit ADC.

2.4 Time-to-Digital conversion

CLICK-B/C has two different receivers. One is based around an Analog to Digital Converter (ADC), with a matched filter, the other is using a Time-to-Digital Converter (TDC). While the ability to measure the transmitted signal on the ADC is useful, we will focus on the TDC receiver, where the loop-back provides timing calibration. The TDC receiver is composed of an analog front end, the TDC itself (a TDC-GPX-2), and a timestamp processing pipeline.

The analog front-end transforms the analog signals from the APD detector into logic-level pulses compatible with the TDC. The pulse is sampled by two comparators. These comparators have been selected based on the lowest slew rates and overdrive dispersion, in order to limit the effects of variations in the pulses amplitude on

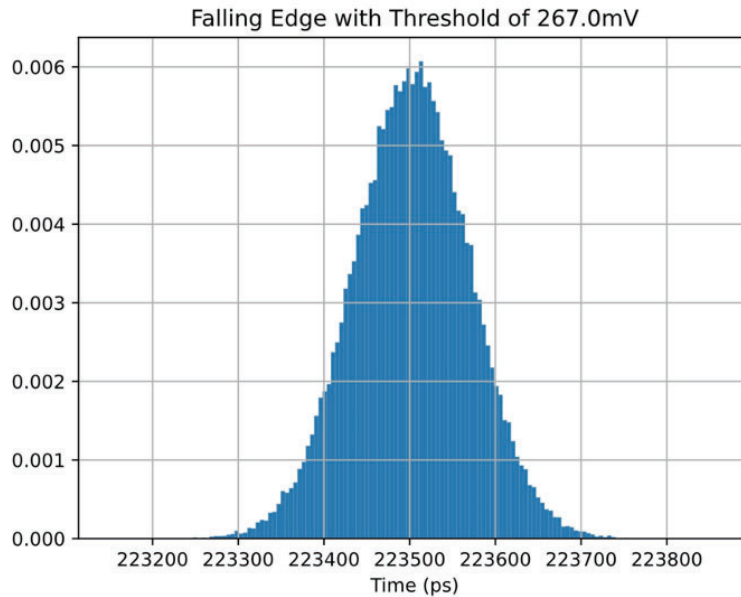


Figure 2: Histogram of time between pulse recorded by the TDC⁵

the timing measurements. The comparators' thresholds are adjustable. The two comparators are followed by four monostable latched, sensing both the rising and falling edges for the two thresholds. All four signals are sensed by the TDC, on the four available channels, providing a way to compensate for time walk, the shift in time due to change in pulse amplitude introduced by thresholding. The TDC samples are sent to the payload Field Programmable Gate Array (FPGA), where the timestamp processing pipeline is implemented. The timestamps are first grouped together, to make sure each set of 2 or 4 timestamps correspond to a single received pulse. The timestamps are then combined in order to cancel time walk. This unique timestamp is sent to a novel, feedback based decoder capable of extracting both data and timing simultaneously. The feedback decoder will be described in detail in future work. <https://www.overleaf.com/project/63022379e9ea9f043fb05c2f>

Characterization of the TDC is ongoing. Initial results with a 4.5 MHz clock fed to one of the TDC channel are shown in fig. 2. The histogram shows the delay between the pulse, and has a full-width, half maximum (FWHM) of approximately 180 ps. The 1σ , single shot precision is better than 55 ps.

3. SELF-CALIBRATION

3.1 Error sources

The transmitter and receiver are optimized for communication, and as such have characteristics that make them less desirable for time-transfer and ranging operations. Both operate with electrical bandwidth much higher than typical for laser time transfer systems. The pulse duration for the transmitter, at 10 ns, is much longer than the pulses typically produced by Q-switched lasers used in satellite laser ranging and optical time transfer. The detector is operating in linear mode, as opposed to Geiger mode, and is susceptible to time walk while the single photon detectors are not. Finally, the receiver and transmitter amplifications and signal conditioning chains are much longer. Where the pulse from single photon detectors can be sampled directly, the analog signal from the data receiver must be amplified to a consistent level and filtered in order to be decoded optimally. Amplifiers introduce delays and noise, that are functions of environmental conditions such as temperature, voltage, radiation and aging. Conversely, communication systems can operate at a much higher pulse rates, in excess of 10^6 faster than previous time transfer systems.⁶ This opens great opportunities using averaging, with the prospect of reaching unprecedented precision for a direct detection system. The problem is then accuracy, how to measure and compensate for the delays and their variations in the system

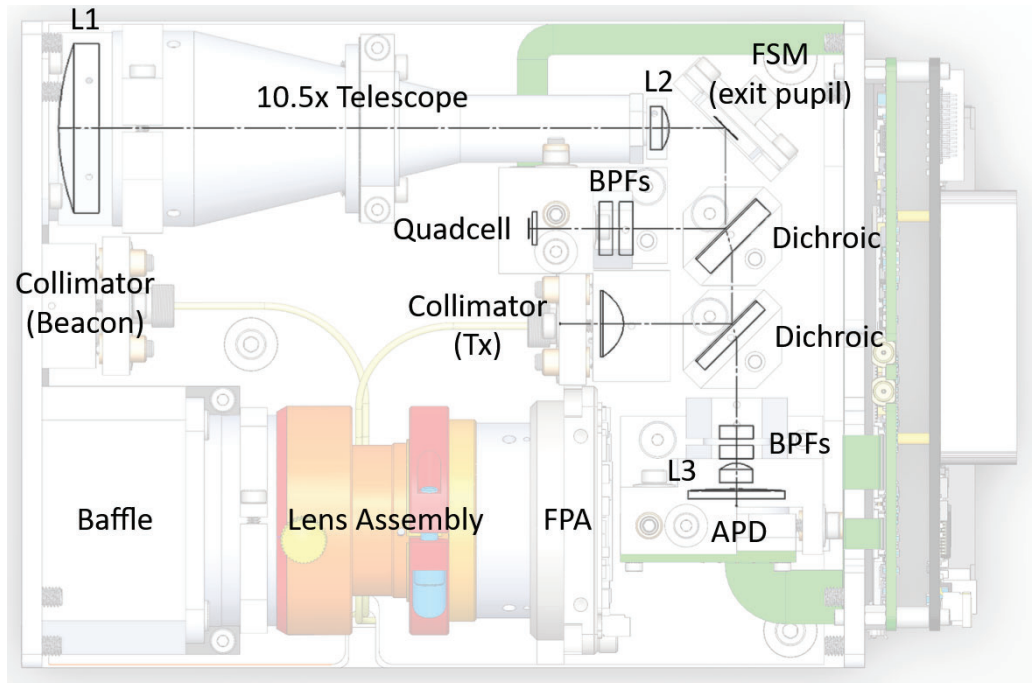


Figure 3: Layout of the CLICK-BC optical bench. Transmitted light is launched by the collimator in the center, reflected on the first dichroic, transmitted through the second dichroic, reflected on the Fine Steering Mirror⁷ (FSM), and finally exits through the telescope. A fraction of the light is reflected by the L2 lens, goes through both dichroics, and reaches the APD.

3.2 Calibration operations

CLICK-B/C is using a single telescope and aperture for data transmission, reception, and fine pointing measurements.^{8,9} Since part of the optical path is shared between data sent and received, the optical design has carefully considered RX/TX isolation, using filtering. The paths are separated using a dichroic beam splitter, and the APD receiver is protected by a two stacked filter, providing 80 dB of attenuation at the transmitter wavelength. The main source of TX to RX crosstalk is the reflection off the telescope L1 and L2 lenses. The anti-reflection coating on each lens is expected to send 0.05 to 0.15 % of the transmitted light into the payload, for a total of 0.1 to 0.3% depending on the wavelength. This is up 600 μ W. The reflected power is then attenuated by the dichroic splitter on the return path, sending the majority of the light back toward the transmit collimator, and 1 % to the APD detector. 60 μ W reach the APD filters at worst, attenuated to 0.6 pW. The reflection off the lenses is not expected to be collimated anymore, due to the lens's spherical surface, and the final estimated power for TX to RX cross-talk is expected to be lower due to this defocus. Furthermore, the reflection on the larger lens, L1, is coming from a divergent beam, and the reflection is expected to be negligible compared to L2.

The optical powers have been measured using an integration sphere at the APD location on the optical bench. The resulting optical power is shown in fig. 4a for a range of wavelengths, including the nominal transmit and receive wavelengths for this unit. In addition, an estimation of the expected power is also plotted. The estimate is based on the Reflectivity of the dichroic splitter R_D and of the L2 lens anti-reflection coating R_{AR} , as well as the transmitted power P_{TX} :

$$P_{est} = R_D \cdot R_{AR} \cdot (1 - R_D) \cdot P_{TX} \quad (3)$$

While the expected shape is apparent, and confirms that the reflection is happening after the dichroic and likely on the L2 lens, the results are shifted by 5 nm. This can be explained by a misalignment of the dichroic. Since the light is incident on the dichroic with a 45° angle, small misalignment can produce a large shift in wavelength.

$$\lambda_{45^\circ+\delta} = \lambda_{45^\circ} [\cos(\delta) + \sin(\delta) \tan(45^\circ + \delta)] \quad (4)$$

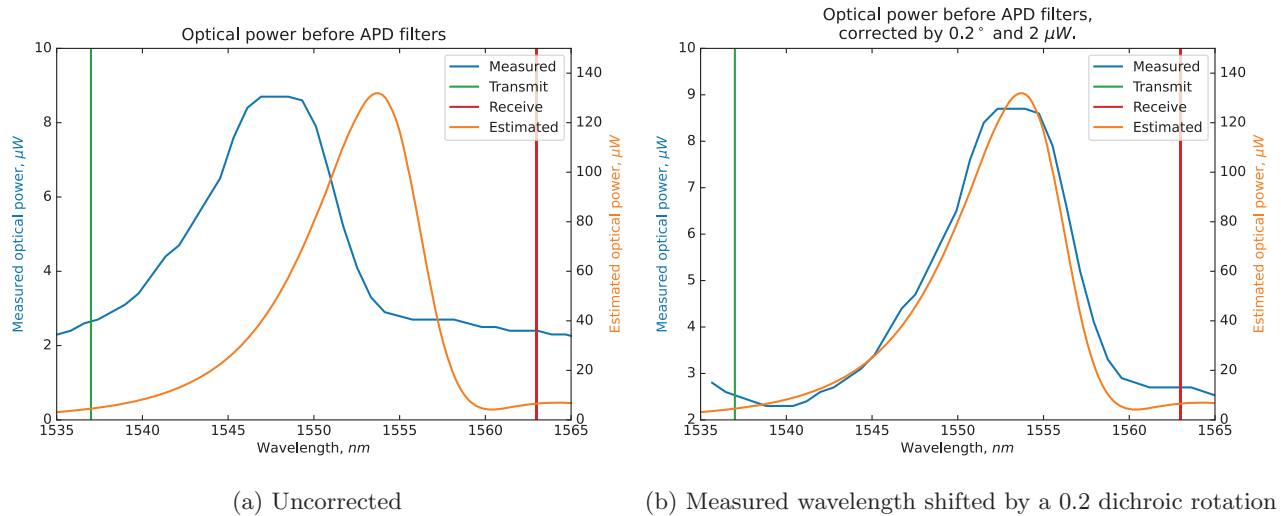


Figure 4: Measured and estimated optical power at the APD detector location, before the APD filters.

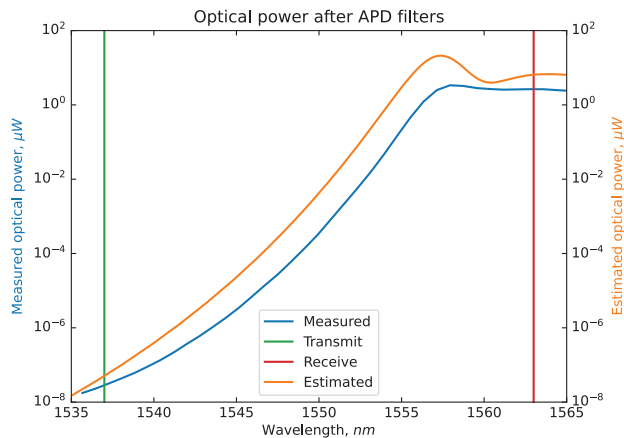


Figure 5: Measured and estimated optical power, both with the simulated effect of the APD filters.

With a misalignment of 0.2° taken into account, and after taking into account a $2\ \mu\text{W}$ offset due to other reflections, the resulting corrected measured optical power is shown in fig. 4b. The modeled and measured power are similar after correction, indicating that the reflection is from the lens anti-reflection coating.

The reflected light then goes through the pair of stacked APD filters, whose impact has been estimated by the filter specifications, and the results are displayed in fig. 5. The power of the reflected signal ranges from $0.01\ \text{pW}$ to $20\ \mu\text{W}$ for the estimate, and $4\ \mu\text{W}$ for the measured power. This range nearly covers both the lowest detectable signal, at $18\ \text{nW}$, and the highest expect signal, at $6\ \mu\text{W}$,¹⁰ when the spacecraft are 25 km apart. By adjusting the transmit wavelength, it is possible to dial in different amounts of power depending on the link conditions. Matching the received power at the APD allows the optical loop-back to operate without changing any of the APD parameters, like bias voltage, amplifier gain, and comparator thresholds. These parameters are kept constant between normal receive operations and calibration operations to minimize their impact, increasing accuracy.

4. CONCLUSIONS AND FUTURE WORK

The CLICK-B/C payload can calibrate its own internal delays by measuring optical pulses reflected inside the payload because the transmit and receive paths share a telescope and aperture. The laser wavelength tuning range is sufficient to achieve the varying TX/RX isolation necessary to perform both crosslink operation and self calibration. During crosslinked data and time transfer, the laser is tuned for high RX/TX isolation. During calibration, the laser is tuned so that cross-talk levels are made similar to received power levels. Further validation of the self-calibration is required, with a completed optical bench, and using the signal of the APD detector directly. On-orbit, real-time calibration of the payload internal time delays will enable an increased accuracy of the system ranging and time transfer, and increase the utility of the precision brought by the high pulse rate. Protocols and payload software are under development to allow automatic, continuous calibration.

ACKNOWLEDGMENTS

The CLICK mission is a collaboration between the MIT Space, Telecommunications, Astronomy, and Radiation (STAR) Lab, University of Florida's Precision Space Systems Lab (PSSL), and NASA Ames Research Center (ARC). This work was funded by the CLICK (CubeSat Laser Infrared CrosslinK) Technology Demonstration Mission, Grant Number 80NSSC18K1579. The views, opinions, and/or findings contained in this work are those of the authors and should not be interpreted as representing the official views or policies, either expressed or implied, of the National Aeronautics and Space Administration.

REFERENCES

- [1] Kingsbury, R., *Optical Communications for Small Satellites*, PhD thesis, Massachusetts Institute of Technology (2015).
- [2] Clements, E., Aniceto, R., Barnes, D., Caplan, D., Clark, J., del Portillo, I., Haughwout, C., Khatsenko, M., Kingsbury, R., Lee, M., Morgan, R., Twichell, J., Riesing, K., Yoon, H., Ziegler, C., and Cahoy, K., "Nanosatellite optical downlink experiment: design, simulation, and prototyping," *Optical Engineering* **55**, 111610 (Sept. 2016).
- [3] Riesing, K., Yoon, H., and Cahoy, K., "A portable optical ground station for low-earth orbit satellite communications," in [*2017 IEEE International Conference on Space Optical Systems and Applications (ICSOS)*], 108–114 (2017).
- [4] Serra, P., Cierny, O., Diez, R., Grenfell, P., Gunnison, G., Kammerer, W., Kusters, J., Payne, C., Murphy, J., Sevigny, T., do Vale Pereira, P., Yenchesky, L., Cahoy, K., Clark, M., Ritz, T., Coogan, D., Conklin, J., Mayer, D., Hanson, J., and Stupl, J., "Optical Communications Crosslink Payload Prototype Development for the Cubesat Laser Infrared CrosslinK (CLICK) Mission," in [*Proceedings of the 33rd AIAA/USU Conference on Small Satellites, SSC19-VI-04*], (2019).
- [5] Coogan, D., Conroy, J., Clark, M., Conklin, J., Tomio, H., Grenfell, W. K. P., Cierny, O., Lindsay, C., Garcia, M., Serra, P., Cahoy, K., Stupl, J., Mayer, D., and Hanson, J., "Development of CubeSat Spacecraft-to-Spacecraft Optical Link Detection Chain for the CLICK-B/C Mission," in [*Proceedings of the 34th AIAA/USU Conference on Small Satellites, SSC20-WKVI-02*], (2022).
- [6] Conklin, J., Nydam, S., Ritz, T., Barnwell, N., Serra, P., Hanson, J., Nguyen, A., Priscal, C., Stupl, J., Jaroux, B., and Zufall, A., "Preliminary Results from the CHOMPTT Laser Time-Transfer Mission," in [*Proceedings of the 33rd AIAA/USU Conference on Small Satellites, SSC19-VI-03*], (2019).
- [7] Mirrorcle Technologies Inc., "Bonded Mirror Devices."
- [8] Yenchesky, L., Cierny, O., Grenfell, P., Kammerer, W., Do, P., Periera, V., Sevigny, T., and Cahoy, K., "Optomechanical Design and Analysis for Nanosatellite Laser Communications," in [*Proceedings of the 33rd AIAA/USU Conference on Small Satellites, SSC19-XII-05*], (2019).
- [9] Tomio, H., Serra, P. C., Cierny, O., Kammerer, W., Grenfell, P., Gunnison, G., Kusters, J., Payne, C., do Vale Pereira, P., Mayer, D., Stupl, J., Hanson, J., Barke, S., Clark, M., Ritz, T., Coogan, D., Conklin, J., and Cahoy, K. L., "CubeSat laser infrared crosslinK mission status," in [*International Conference on Space Optics — ICSO 2020*], Cugny, B., Sodnik, Z., and Karafolas, N., eds., **11852**, 118523D, International Society for Optics and Photonics, SPIE (2021).

- [10] Grenfell, P., Serra, P., Cierny, O., Kammerer, W., Gunnison, G., Kusters, J., Payne, C., Cahoy, K., Clark, M., Ritz, T., Coogan, D., Conklin, J., Mayer, D., Stupl, J., and Hanson, J., “Design and Prototyping of a Nanosatellite Laser Communications Terminal for the Cubesat Laser Infrared CrosslinK (CLICK) B/C Mission,” in [*Proceedings of the 34th AIAA/USU Conference on Small Satellites, SSC20-WKVI-02*], (2020).